J. Microbiol. Biotechnol. (2016), 26(11), 1908–1917
http://dx.doi.org/10.4014/jmb.1604.04019

jmb

Enhancement of 1,3-Dihydroxyacetone Production from *Gluconobacter oxydans* by Combined Mutagenesis S

Xi Lin†, Sha Liu†, Guangrong Xie†, Jing Chen, Penghua Li, and Jianhua Chen*

School of Life Science and Technology, China Pharmaceutical University, Nanjing 210009, China

Received: April 7, 2016
Revised: July 16, 2016
Accepted: July 20, 2016

**Corresponding author*
Phone: +86-025-86185249;
Fax: +86-025-83271290;
E-mail: chenjhnj@163.com

†These authors contributed equally to this work.

Supplementary data for this paper are available on-line only at http://jmb.or.kr.

pISSN 1017-7825, eISSN 1738-8872

Wild strain L-6 was subjected to combined mutagenesis, including UV irradiation, atmospheric and room temperature plasma, and ion beam implantation, to increase the yield of 1,3-dihydroxyacetone (DHA). With application of a high-throughput screening method, mutant *Gluconobacter oxydans* I-2-239 with a DHA productivity of 103.5 g/l in flask-shake fermentation was finally obtained with the starting glycerol concentration of 120 g/l, which was 115.7% higher than the wild strain. The cultivation time also decreased from 54 h to 36 h. Compared with the wild strain, a dramatic increase in enzyme activity was observed for the mutant strain, although the increase in biomass was limited. DNA and amino acid sequence alignment revealed 11 nucleotide substitutions and 10 amino acid substitutions between the *sldAB* of strains L-6 and I-2-239. Simulation of the 3-D structure and prediction of active site residues and PQQ binding site residues suggested that these mutations were mainly related to PQQ binding, which was speculated to be favorable for the catalyzing capacity of glycerol dehydrogenase. RT-qPCR assay indicated that the transcription levels of *sldA* and *sldB* in the mutant strain were respectively 4.8-fold and 5.4-fold higher than that in the wild strain, suggesting another possible reason for the increased DHA productivity of the mutant strain.

Keywords: 1,3-Dihydroxyacetone, glycerol, bioconversion, fermentation, enzyme activity, combined mutagenesis

Introduction

1,3-Dihydroxyacetone (DHA) has been widely used as a precursor for synthesizing many fine chemicals in the chemical industry and as an active browning ingredient in the cosmetic industry [3, 7, 27]. Compared with chemical synthesis, the biotechnical way of DHA production is characterized by low cost and environmental friendliness. A variety of microorganisms can convert glycerol into DHA by glycerol dehydrogenase, such as *Gluconobacter oxydans* [15], *Escherichia coli* [34], *Klebsiella aerogenes* [26] and *Gluconacetobacter xylinus* [4], among which *G. oxydans* is most widely used in DHA production at the commercial scale. The complex biosynthesis of DHA by *G. oxydans* was reported to involve membrane-bound glycerol dehydrogenase (GLDH, E.C. 1.1.99.22). The catalyzing enzyme was first purified and characterized by Ameyama *et al.* [2]. As a quinoprotein, GLDH contains pyrroloquinoline quinone (PQQ) functioning as the prosthetic group. Many polyhydroxyl alcohols have been proved as the substrates of GLDH, including mesoerythritol, propylene glycol, D-mannitol, D-arabitol, D-sorbitol, and adonitol [16].

The increasing demand of DHA in recent years has promoted a surge of investigations and studies on enhancement of DHA production. In addition to improvement in fermentation processes [10, 11, 24], mutation breeding of DHA-overproducing strains is also an effective method for increasing DHA production. Conventional methods of mutagenesis, like ultraviolet irradiation and microwave mutation, as well as newly developed methods, like He-Ne laser irradiation technology and ion beam implantation, have been applied to breed DHA-overproducing strains. In the study by Hu and Zheng [15], UV-induced mutant *G. oxydans* ZJB11001 achieved about 40 mg/ml DHA production after 64 h of shake-flask fermentation. In another study also by Hu *et al.* [13], *G. oxydans* ZJB09113

obtained after ion beam implantation displayed DHA production of 13.8 mg/ml. The newly isolated strain *Gluconobacter frateurii* CGMCC 5397 by Liu *et al.* [19] achieved a DHA concentration of 73.1 mg/ml in shake-flask fermentation. In the study by Ma *et al.* [20], a DHA concentration of 86.33 mg/ml was achieved in shake flask by mutant *G. oxydans* obtained after He–Ne laser irradiation. Nevertheless, the DHA productivity achieved by those mutant strains was still not enough to meet industrial demand.

As a new plasma-generating system, atmospheric and room temperature plasma (ARTP) enjoys the advantages of low cost, feasible operations, harmlessness, and higher mutational possibility, holding great promise in biotechnological application [30]. The ARTP mutation breeding system was first successfully applied in the mutagenesis of *Streptomyces avermitilis* to generate mutants with high productivity of avermectins in 2009 [29]. Since then, the ARTP mutagenesis method has attracted extensive attention from researchers and been further applied in strain breeding to increase the bioproductivity of various chemicals, including butanol [9], epsilon-poly-L-lysine [35], and succinic acid [18]. Because of the high total and positive mutation rate as well as high hereditary stability of the resultant mutants, ARTP breeding is expected to be more extensively applied in strain modification. However, application of ARTP in mutation breeding for DHA production has not been reported.

In this study, a DHA-producing strain screened from soil samples was subjected to combined mutagenesis, including UV irradiation, ARTP, and ion beam implantation. A mutant with significantly improved productivity and genetic stability was obtained. Analysis of the biomass, mutation sites, and transcription level of the converting enzyme revealed possible reasons for the increased DHA productivity from the mutant strain.

Materials and Methods

Bacterial Strain, Media Composition, and Cultivation Conditions

The starting strain L-6 was isolated by screening a soil sample and stored at 4°C on agar slant (yeast extract, 5 g/l; glucose, 20 g/l; glycerol, 20 g/l; $CaCO_3$, 5 g/l; agar powder, 20 g/l).

For DHA production, cells from the agar slant were first inoculated into 100 ml of seed medium (yeast extract, 5 g/l; glucose, 20 g/l; glycerol, 20 g/l) in a 500 ml flask. After cultivation at 30°C and 200 rpm for 24 h, 2.5 ml of inoculum was transferred into a fermentation medium (yeast extract, 5 g/l; $MgSO_4 \cdot 7H_2O$, 0.1 g/l; $CaCO_3$, 2 g/l; glycerol, 80–120 g/l; depending on the mutagenesis method). DHA production was completed after cultivation at 30°C and 200 rpm for 36–54 h (depending on the producing strain).

Strain Identification

According to *Bergey's Manual of Sytematic Bacteriology*, morphological and biochemical characterization were performed [5]. 16S rDNA was amplified from total genomic DNA by using primers 5′-AGAGTTTGATCCTGGCTCAG-3′ (forward) and 5′-ACGGCT ACCTTGTTACGATTT-3′ (reverse). The PCR system contained 37.0 µl of ddH_2O, 4 µl of 4×dNTP mix, 5 µl of 10×Taq Plus buffer, 0.5 µl of 50 µmol/l primers, 3 µl of genomic DNA, and 0.5 µl of Taq DNA polymerase. The amplification program was as follows: denaturation at 95°C for 5 min; followed by 30 cycles of 95°C for 30 sec, 55°C for 1 min, 72°C for 2 min; and final extension at 72°C for 10 min. The amplified fragments were sequenced and then aligned with homologous sequences from the GenBank database using the ClustalX software. A phylogenetic tree was constructed by the neighbor-joining method using the MEGA 3.1 software.

Mutagenesis Program

UV irradiation. The broth of starting strain L-6 obtained after cultivation to logarithmic phase was diluted and spread on agar plates. The plates were then irradiated under a UV lamp (18 W) for 0–210 sec to determine the survival rate and rate of positive mutation at different exposure times. UV irradiation was conducted for several rounds until positive mutants could be sparsely screened. The media for high-throughput screening and shake-flask fermentation contained 80 g/l glycerol.

Atmospheric and room temperature plasma. The mutant strain showing the highest DHA productivity and good hereditary stability after UV irradiation was further subjected to ARTP mutagenesis. The ARTP mutation breeding system (Siqingyuan, China) contains a plasma generator that can eject helium plasma consisting of different reactive species, such as oxygen atom lines, helium lines, N_2 lines, and hydroxyl (OH) molecular band [17]. First, 1 ml of bacteria culture at logarithmic phase was transferred into a sterile tube and diluted with sterile saline to reach OD_{600} of 1~2. Then, 10 µl of the diluted culture was dropped onto a stainless plate and dried for 20–30 min in sterile air, and then exposed to the jet nozzle exit at a distance of 2 mm. The facility was operated under the RF power of 100 W, at the helium flow rate of 10 standard liters per minute, and time of exposure of 0 to 240 sec, with an interval of 30 sec. After exposure, the sample plate was immersed into sterile water to wash off the bacteria. The resulting bacterial suspension was spread on an agar plate for selection of single colonies and screening of high-producing strains. ARTP mutagenesis was repeated for several rounds until positive mutants could be sparsely screened. The media for high-throughput screening and shake-flask fermentation contained 100 g/l glycerol.

Ion beam implantation. A 0.1 ml sample of bacteria broth at logarithmic phase was spread on a sterile petri dish and air-dried in a biosafety cabinet. The dish was then placed in the target chamber and implanted with the N^+ ion beam under a dry

vacuum station [23]. The energy and dose of N^+ ion beam implantation were fixed at 10 keV and 0–30 × (2.6×10^{13}) ions/cm^2. After ion beam implantation, the cells were harvested using sterile saline water and spread onto an agar plate. Mutagenesis by the N^+ ion beam was repeated for several rounds until positive mutants could be sparsely screened. The media for high-throughput screening and shake-flask fermentation contained 120 g/l glycerol.

Evaluation of Survival Rate and Positive Mutation Rate

The survival rate was calculated according to the following equation: survival rate = (C_1/C_0) × 100%, where C_1 is the number of clones on the plate after treatment with mutagen, and C_0 is the number of clones on the control plate without treatment. The positive mutation rate was calculated according to the following equation: positive mutation rate = (M_1/M_0) × 100%, where M_1 is the number of clones that develop a more intense color on the high-throughput screening microtiter plate than the parent strain; and M_0 is the number of clones on the plate after treatment with mutagen.

Screening for DHA-Overproducing Mutants

Mutants with significantly increased productivity were screened with a high-throughput method as described previously [14]. Briefly, the starting strain as well as single colonies on the agar plate after mutagenesis were inoculated into the corresponding well of duplicate 96-well microtiter plates (plate X and Y) filled with 0.2 ml of medium (yeast extract, 5 g/l; agar powder, 1.5 g/l; glycerol, 80–120 g/l; depending on the mutagenesis method). The plates were then incubated at 30°C for 24 h. Then, 60 µl of Fehling's reagent was added to each well of plate X and incubated at 25°C for 15 min. A yellow-red color developed in the presence of DHA and a more intense color than the well of the starting strain indicated a positive mutation. Positive mutants were confirmed by fermentation in 500 ml shake flasks.

DHA and Glycerol Assay

A high-performance liquid chromatography (HPLC) method developed by Chen *et al*. [6] was used to determine DNA. A Lichrospherb 5–NH_2 column (Jiangsu Hanbon Science & Technology Co. Ltd) was operated at 30°C in an Agilent 1000 system with a UV detector set at 271 nm. The mobile phase constituted acetonitrile-water (90:10 (v/v)) at a flow rate of 1.0 ml/min. Glycerol was assayed in the same chromatographic condition except that a differential refractometer detector was used. Standard curves with good linearity were first established in the range of 2.00–12.00 mg/ml and 0.5–50 mg/ml for DHA and glycerol, respectively.

Mutant Strain Stability

For the positive mutants with significant increase in DHA productivity after each round of mutagenesis, their hereditary stability was investigated by continuous subcultures. The slant of a mutant isolate was cultivated at 30°C for 48 h and then subcultured to a new slant, which was also cultivated at 30°C for 48 h. Totally, 10 subsequent subcultures were performed. Bacteria of each passage were transferred into a shake flask to determine DHA productivity. The mutants obtained from the same mutagenesis method were cultured under the same condition to determine DHA productivity. Only mutants with both high productivity and hereditary stability were sent to the next round of mutagenesis.

Comparison between Starting Strain L-6 and Mutant Strain I-2-239

Biomass. Biomass was determined by cell dry weight. After centrifugation at 8,000 rpm for 10 min, cells from 50 ml of culture were washed with distilled water for 3–4 times and dried to constant weight at 105°C.

Enzymatic activity. The activity of the catalyzing enzyme was determined as described by Nabe *et al*. [22]. Cells at logarithmic phase were collected by centrifugation at 10,000 rpm for 10 min and washed with phosphate buffer (pH 6.0). About 100 mg of intact cells of wild strain L-6 and the mutant strain I-2-239 were respectively suspended in 1 ml of phosphate buffer (pH 6.0) and then added into 50 ml of 100 mg/ml glycerol in a 500 ml shake flask. After incubation at 30°C and 200 rpm for 3 h, the conversion was stopped by removing the cells by centrifugation, followed by determination of DHA in the resultant supernatant by HPLC. Enzyme activity was expressed in terms of micromoles of DHA produced per hour.

Structural Modeling and Mutant Sites Analysis

Genomic DNA of starting strain L-6 and mutant strain I-2-239 was extracted according to the instructions for the bacterial genomic DNA extraction kit (Tiangen, China). The primers for glycerol dehydrogenase gene (*sldAB*) amplification were 5′-CCGCTCGAGATGCCGAATACTTATG-3′ (forward) and 5′-ACG GCTACCTTGTTACGATTT-3′ (reverse). The reaction system contained 5 µl of 10×Taq Plus buffer, 37.0 µl of ddH_2O, 4 µl 4×dNTP mix, 0.5 µl of 50 µmol/l primers, 0.5 µl of Taq DNA polymerase, and 3 µl of genomic DNA. The PCR amplification program was as follows: denaturation at 95°C for 5 min; followed by 30 cycles of 95°C for 30 sec, 55°C for 1 min, 72°C for 170 sec; and final extension at 72°C for 10 min. After digestion with EcoRI/HindIII, the target gene was ligated to pUC-19 plasmid for sequencing. The *gldh* sequence of strain L-6 was aligned with that of the mutant strain I-2-239.

The structure of wild sldA (the functional polypeptide of glycerol dehydrogenase) from strain L-6 as well as its active site and ligand binding site was predicted using the online I-TASSER server (http://zhanglab.ccmb.med.umich.edu/I-TASSER/). The generated model was evaluated and validated using the Structural Analysis and Verification Server (SAVES). A Psi/Phi Ramachandran plot was obtained using PROCHECK to check the amino acid residues at disallowed regions. VERIFY-3D was used to evaluate the 3D-1D score of the model.

Table 1. Primer sequences for the RT-PCR test.

	Forward primer	Reverse primer
16S rRNA	GCGGTTGTTACAGTCAGATG	GCCTCAGCGTCAGTATCG
sldA	CCTGCGTAGCCCTGAAGAAAAC	CGAGCCGATGTCATAGTCCC
sldB	CAGCAGAACCCTGACCG	GGAATGCCACAGATGACG

Transcription Assay

The transcription levels of the two polypeptides sldA and sldB of glycerol dehydrogenase were compared between strain L-6 and strain I-2-239 by using RT-qPCR. Total RNA of both strains were isolated using TRIeasy Total RNA Extraction Reagent (Yeasen Biotech, China). DNase treatment was performed on the eluted RNA to avoid residual DNA contamination. Reverse transcriptase was performed using the PrimeScript First Strand cDNA Synthesis Kit (Takara). Primers based on *sldA*, *sldB*, and 16S rRNA were designed using Primer Premier Software (ver. 5.0; Premier Biosoft International, USA), as shown in Table 1. Quantitative RT-PCR was performed on the Step One Plus System (Applied Biosystems, USA) in a 20 µl volume containing 1× SYBR Green Master Mix (Vazyme, China), 50 ng of cDNA, and 0.4 µM primers. Thermal cycling conditions were 95°C for 5 min, and 40 cycles of 95°C for 10 sec and 60°C for 30 sec. All reactions were performed in triplicates. Target gene expression in each sample was normalized to the endogenous control gene 16S rRNA. The $2^{-\Delta\Delta CT}$ method was employed to report the mean fold-change in transcripts.

Results and Discussion

Identification of Isolate L-6

Morphological characterization indicated that isolate L-6 was gram negative, aerobic, rod shaped, and without production of pigment. Its colonies were milky white, round, and with irregular edges. By chemical test, the isolate was negative for indole production, nitrate reduction, gelatin liquefaction, and H_2S formation, but positive for catalase. Based on these morphological and physiological characteristics, strain L-6 was preliminarily identified as *G. oxydans*. A maximum DHA productivity of 47.98 mg/ml was attained after cultivation at 30°C and 200 rpm for 54 h.

The 16S rDNA of strain L-6 was amplified and sequenced, and a fragment of 1,345 bp was obtained. Sequence homology revealed that L-6 strain was related to members of genus *Acetobacter* and showed highest sequence similarity to *G. oxydans* (99% identity). The sequence was aligned using the ClustalX software to nine 16S rDNA sequences retrieved from the GenBank database, and a phylogenetic tree (Fig. 1) was constructed using the MEGA 3.1 software. The phylogenetic tree indicated that strain L-6 together with *G. oxydans* 621H (Accession No. NR_074252.1) and *G. oxydans* JR70-1 (Accession No. AB436557.1) formed a distinct linkage in the tree with 96% bootstrap support. The L-6 strain was identified as *G. oxydans*.

Screening DHA-Overproducing Mutants

Ultraviolet is an easily accessible approach for screening

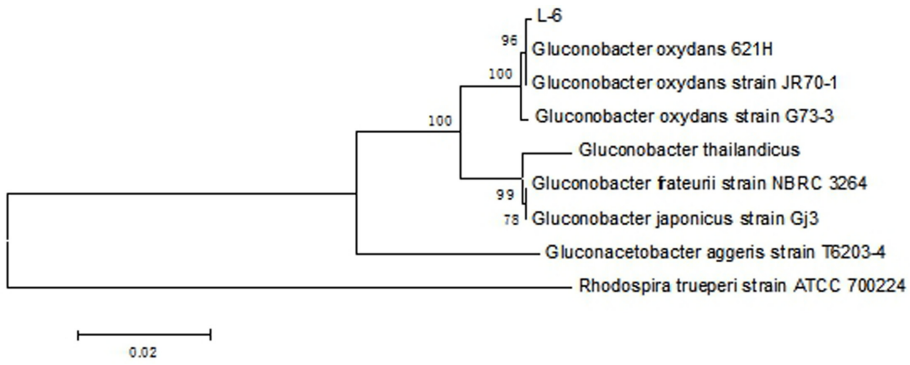

Fig. 1. Phylogenetic tree based on 16S rDNA sequences of strain L-6 and other related bacteria.

Reference sequences were retrieved from GenBank and their accession numbers are as follows: NR_074252.1 (*G. oxydans* 621H), AB436557.1 (*G. oxydans* strain JR70-1), HM217965.1 (*G. oxydans* strain G73-3), NR_113920.1 (*Gluconobacter thailandicus* strain F149-1), NR_112239.1 (*G. frateurii* strain NBRC 3264), JF346080.1 (*Gluconobacter japonicus* strain Gj3), NR_114382.1 (*Gluconacetobacter aggeris* strain T6203-4-1a), and NR_114681.1 (*Rhodospira trueperi* strain ATCC 700224). Numbers on the branches represent bootstrap values for 1,000 replicates. *Rhodospira trueperi* strain (ATCC 700224) was used as the outgroup.

high-yield strains for industrial application. As illustrated in Fig. 2, the survival rate declined with the increase in exposure time, and a survival rate lower than 10% was achieved after exposure for 90 sec. The highest rate of positive mutation was obtained after exposure for 120 sec. Three rounds of UV-induced mutations were performed and approximately 1,000 mutants were screened. A significantly decreased rate of positive mutations in the third mutation round indicated that the maximum potential of UV-induced mutation was achieved. After hereditary stability study, strain U-2-115 with DHA productivity of 71.4 g/l in flask culture was obtained, showing a 48.8% increase compared with the starting strain L-6.

U-2-115 was then subjected to ARTP mutagenesis. ARTP-induced mutation has a totally different acting pattern on DNA. The chemical reactive species contained in the plasma jet can destroy the phosphate group in mononucleotides and further break oligonucleotides into fragments, producing a higher positive genotoxic response than traditional rays. The survival rate curve took a saddle shape (Fig. 3), which was different from the shoulder or exponential pattern of the conventional mutagenic method. At fixed instrumentation parameters, 150 sec with the highest rate of positive mutation (26%) was selected as the optimal treatment time. ARTP mutation was conducted for two rounds to achieve the maximum potential of this method. Strain A-2-64 with DHA productivity of 90.2 g/l in flask culture was obtained, showing 26.3% and 87.9% increases compared with strains U-2-115 and L-6, respectively. This is the first reported application of ARTP in strain breeding for DHA production. Because the acting pattern on DNA is different from ultraviolet irradiation, a further increase in DHA productivity was still achieved in strains that had undergone several rounds of UV mutagenesis.

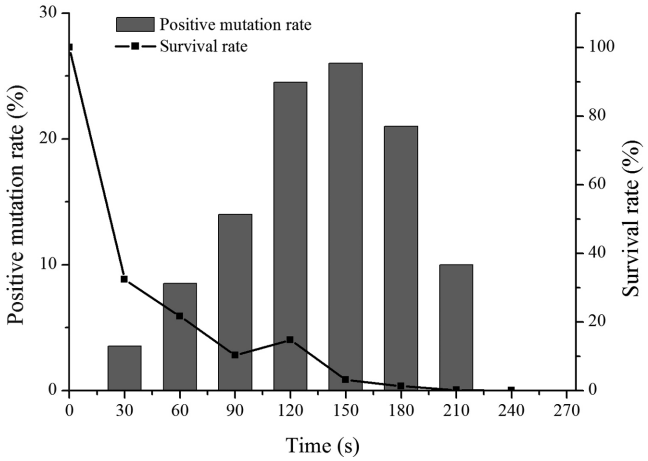

Fig. 3. Survival rate and positive mutation rate of ARTP.

Strain A-2-64 was further subjected to N^+ ion beam implantation, which is characterized by wider mutation spectra for organisms and higher mutation frequency. The possible underlying mechanisms for DNA damage include charge exchange, mass deposition, and energy absorption, causing changes in cell morphology and subcellular structures as well as modifications of biological macromolecules. At fixed energy, the N^+ ion beam implantation dose strongly affects the survival rate. As shown in Fig. 4, the survival rate declined sharply from $0–10 \times 2.6 \times 10^{13}$ ions/cm^2, then slightly increased between $10–20 \times 2.6 \times 10^{13}$ ions/cm^2, and restarted to decline when the dose exceeds $20 \times 2.6 \times 10^{13}$

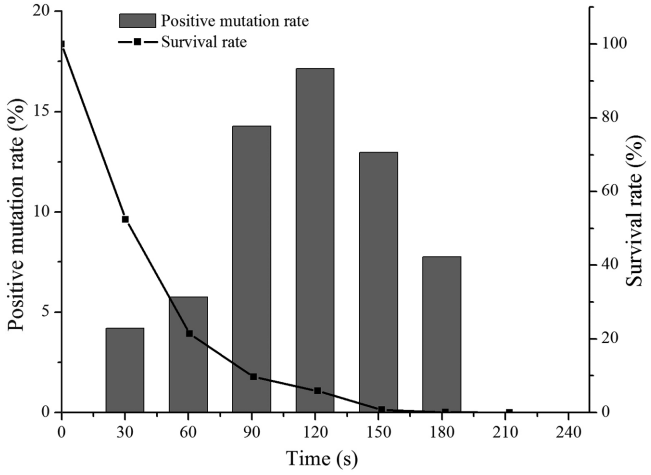

Fig. 2. Survival rate and positive mutation rate of ultraviolet irradiation.

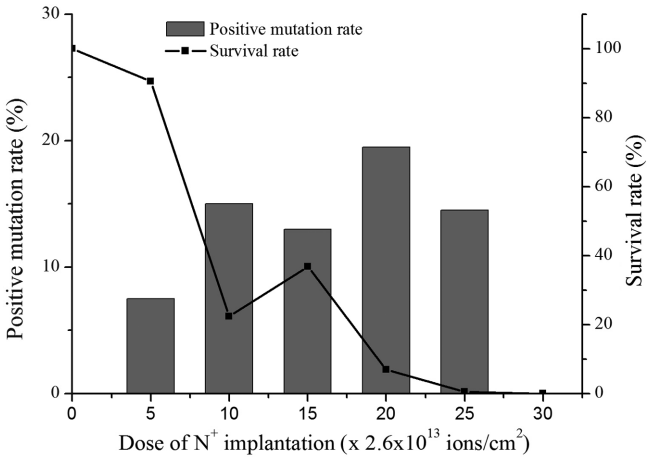

Fig. 4. Survival rate and positive mutation rate of ion beam implantation.

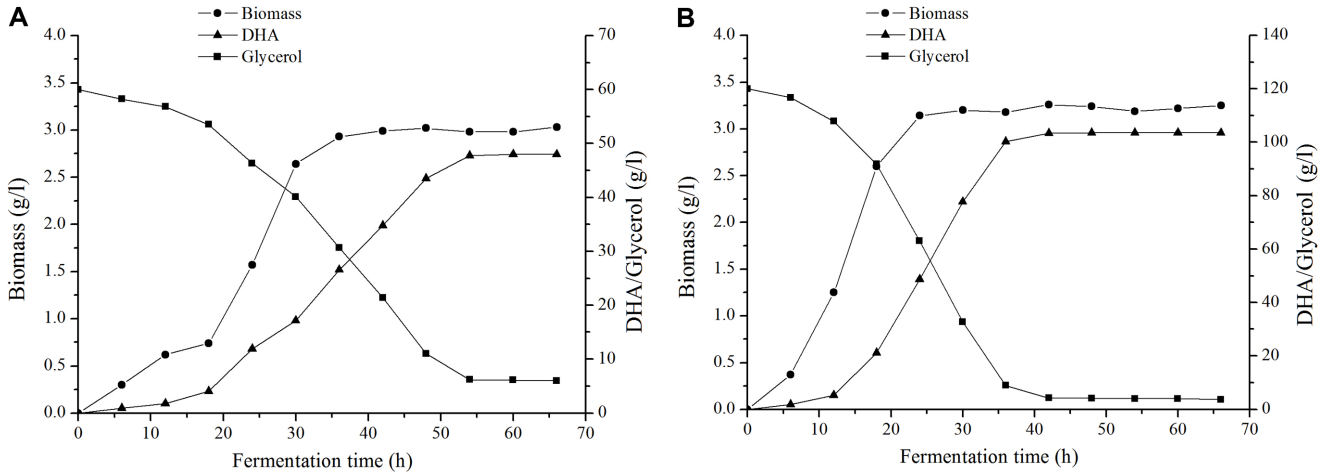

Fig. 5. Fermentation course of strains L-6 (**A**) and I-2-23 (**B**).

ions/cm^2. The 20 × 2.6 × 10^{13} ions/cm^2 dose was selected as the optimal implantation dose in favor of high positive mutation rate. The death curve was very different from the curve reported by Hu *et al.* [13] in the screening of DHA-producing *G. oxydans*. Although the same species of bacteria was mutated by the same method for the same purpose, a much higher resistance to ion beam implantation was observed in the study by Hu *et al.*, in which a survival rate lower than 10% could only be achieved when the dose exceeded 90 × 2.6 × 10^{13} ions/cm^2. It was speculated that the previous mutagenesis by UV irradiation and ARTP in this study to some extent increased the susceptibility of our *G. oxydans* strain to N^+ ion beam implantation. Two rounds of mutagenesis induced by N^+ ion beam implantation were performed. After high-throughput screening, shake-flask fermentation, and hereditary stability study, strain I-2-239 with DHA productivity of 103.5 mg/ml was obtained, showing 14.7% and 115.7% increase compared with strains A-2-64 and L-6, respectively.

The combined mutagenesis in this study included methods with different mechanisms in producing DNA damage and thus produced extra increase in productivity than mutagenesis by any single method. The finally obtained strain I-2-239 displayed a 115.7% increase in DHA yield than starting strain (Table 1). This is also the highest reported DHA production in shake flask fermentation so far, showing significant value in industrial application.

Comparison between Starting Strain L-6 and Mutant Strain I-2-239

DHA production, glycerol residue, and biomass during shake-flask fermentation. When cultivated under the same conditions (60 mg/ml glycerol for strain L-6 and 120 mg/ml glycerol for strain I-2-239), a much higher DHA production was achieved by strain I-2-239 (Fig. 5). Although the biomass of strain I-2-239 has a slight edge over that of the wild strain at the end of fermentation (3.26 g/l vs. 3.03 g/l), a much steeper biomass curve in the exponential phase was observed for strain I-2-239, corresponding to earlier achievement of maximum DHA production than strain L-6 (36 vs. 54 h). These results indicated that the mutations accumulated during the combined mutagenesis did not have significant impact on cell biomass but dramatically increased the growth rate, which was especially advantageous for industrial fermentation.

Enzymatic activity. In order to determine if the catalyzing capacity of GLDH was affected by mutagenesis, the enzymatic activity of resting cells was determined. As shown in Table 2, a higher glycerol-oxidizing activity was observed with the intact cell of strain I-2-239. Since the same cell mass was used for parallel comparison, the increase in enzymatic activity indicated that mutations accumulated in the combined mutagenesis led to increased GLDH expression or to changes in GLDH protein in favor of its catalyzing capacity.

Table 2. Summary of combined mutagenesis.

Mutation program	Mutant strain	DHA production (g/l)	Increase compared with strain L-6(%)
UV	U-2-115	71.4 ± 0.35	48.8
ARTP	A-2-64	90.2 ± 0.25	87.9
Ion beam implantation	I-2-239	103.5 ± 0.54	115.7

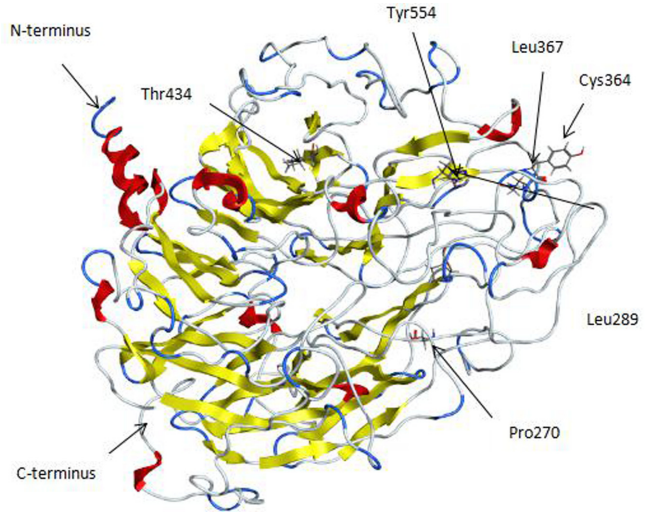

Fig. 6. 3-D structure of sldA in wild strain L-6 generated by I-TASSER.
The α-helix is shown in red, β-sheet in yellow, β-turn in blue, and random coil in gray. Mutated residues are shown by arrows.

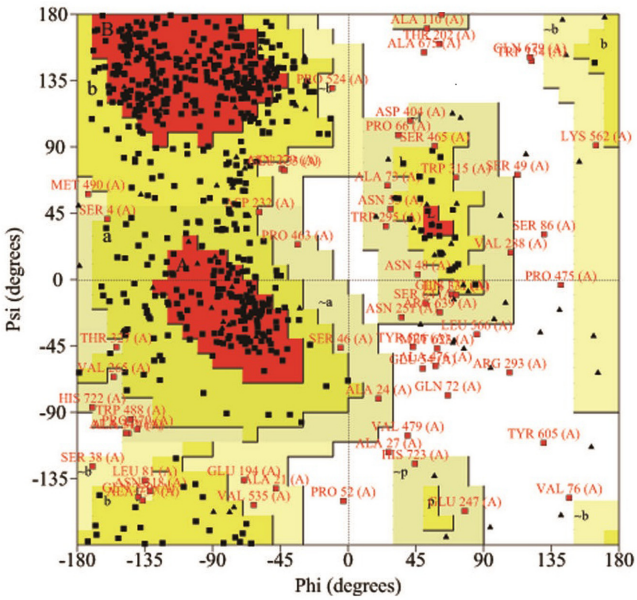

Fig. 7. Ramachandran plot indicating the phi (Φ)-psi (Ψ) torsion angles for all the amino acid residues in the modeled structure of wild sldA.

Structural Modeling and Mutant Sites Analysis

The GLDH genes (*sldAB*) of starting strain L-6 and mutant strain I-2-239 were sequenced. The full-length *sldAB* accounts for 2,612 bp, with 2,232 bp in *sldA* and 381 bp in *sldB*. As shown in Fig. S1, the termination codon of *sldB* overlaps with the initiation codon of *sldA* with 1 bp. *sldB* codes for a 13,723 Da subunit, a hydrophobic polypeptide of 126 residues. *sldA* codes for another subunit of 743 amino acids with a predicted molecular mass of 79,512 Da.

The three-dimensional structure of wild sldA was generated using I-TASSER online server. The top 10 threading templates retrieved from the PDB database and used by I-TASSER all had a relatively low similarly with wild sldA. The highest homology (24%) was observed in alignment with quinohemoprotein alcohol dehydrogenase ADHIIG from *Pseudomonas putida* HK5 [28]. The established model with the highest C-score is shown in Fig. 6. Ten α-helixes and 36 β-sheets can be found in this conformation. The large number of random coils appearing in this model was due to the inadequate homology between the template and the target protein. The Ramachandran plot indicates that the percentages of residues in most favored regions, additional allowed regions, and disallowed regions are 58.0%, 32.4%, and 2.9%, respectively (Fig. 7). Evaluation by VERIFY 3-D indicated that 82.77% of the residues had an average 3D-1D score ≥ 0.2. All these data indicated that the established model is suitable for further analysis. I-TASSER is a hybrid modeling method that includes three conventions for structure modeling; namely, threading, comparative modeling, and ab initio modeling [25]. This method can give confident structure prediction even when crystal structures with high similarity are unavailable [32, 33]. As a result, a reliable model of sldA in the wild strain was generated despite of its low homology with the templates.

DNA sequences alignment of *gldh* in strains L-6 and I-2-239 totally identified 11 nucleotide substitutions in the mutant strain, three in *sldB* and seven in *sldA*. All these substitutions led to changes in amino acid residues except G459A. *sldB* and *sldA* code for the two polypeptides that are required for GLDH activity. Studies have shown that the catalytic activity was from the sldA polypeptide, whereas the sldB polypeptide possibly had a chaperone-like function to assist the folding of sldA polypeptide into an active form [12]. To further analyze the impact of these mutations on enzyme function, the active site residues and PQQ binding site residues of wild sldA polypeptide were predicted by I-TASSER. The predicted active site 402 was not included in these substitutions, predicting that the substitutions in the mutant sldA did not affect the catalytic capacity of the enzyme protein. The predicted PQQ binding site residues included amino acid residues 157, 201, 204, 206, 272, 287, 288, 289, 290, 338, 340, 357, 358, 404, 430, 531, 659, 723, and 724, all in sldA. Although only residue 289 was included in the mutation sites, some other

mutation sites (270, 364, 367, and 434) were very close to the predicted PQQ binding sites. There are two types of glycerol dehydrogenases; one is pyridine nucleotide (NAD^+ or $NADP^+$) dependent and the other is independent and membrane bound. GLDH belongs to the latter type of enzyme, which is covalently bound to the prosthetic group PQQ, a chemical also present in some other bacterial dehydrogenases, including alcohol dehydrogenase, aldehyde dehydrogenase, and glucose dehydrogenase [1]. PQQ is involved in the oxidation-reduction reaction via transferring electrons. We speculated that the substitutions in the mutant sldA polypeptide increased the binding between enzyme protein and the prosthetic group, which was favorable for a more efficient electron transfer and thus an increased catalytic activity.

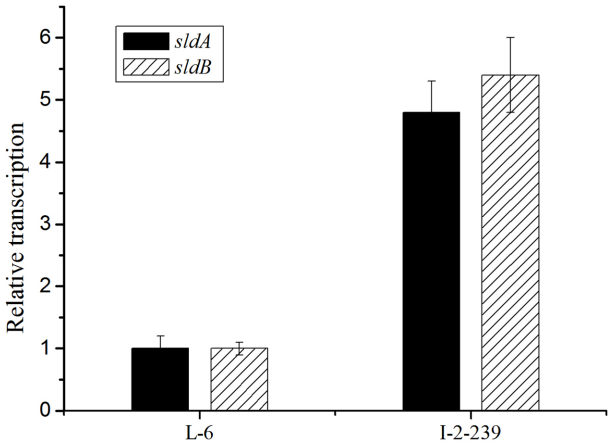

Fig. 8. Mean fold change of sldA and sldB mRNA in strains L-6 and I-2-293.

Transcription Level Analysis

To investigate if the mutations brought any impact on the transcription level of *gldh*, strains L-6 and I-2-239 were collected and subjected to RT-qPCR. Primers were designed against *sldA* and *sldB* to determine their relative transcription compared with endogenous control gene 16S rRNA. Comparison with the wild strain showed 4.8-fold and 5.4-fold increases in the transcription level of *sldA* and *sldB*, respectively, in the mutant strain (Fig. 8). Sequencing of *sldAB* in previous studies [12, 21] and also in our study showed that *sldA* and *sldB* were adjacent, overlapping each other between the termination codon of *sldB* and the initiation codon of *sldA*. The nearly consistent increase in transcription level of *sldA* and *sldB* appeared to support the hypothesis proposed by Hoshino *et al*. [12] that the two genes were likely to be transcribed polycistronically from the upstream of the *sldB* gene. The level of transcription, indicated by the abundance of mRNA, is directly related to enzyme expression and hence to productivity. As reported by Xu *et al*. [31], increased transcription of the sorbitol dehydrogenase gene resulted in improved conversion of L-sorbose from D-sorbitol. When an extra poly(A) tail was introduced at the 3′-end of the mRNA of the sorbitol dehydrogenase gene, its transcription level was more than 6-fold higher than that of the control. A 15.9% improvement in L-sorbose production was obtained in the engineered strain although increase in enzyme activity was not significant [31]. In the study by Cornelia Gätgens *et al.* [8], the glycerol dehydrogenase gene was overexpressed in *G. oxydans*, resulting in increased transcription level of *gldh* and DHA accumulation. In our study, it was speculated that the increased transcription of *sldA* polypeptide enhanced the catalyzing capacity of each cell unit due to the subsequent increase in enzyme expression. Although the sldB polypeptide is not directly involved in catalysis, its increased expression was supposed to be beneficial to the correct folding of the sldA polypeptide, which also accounted for the increased enzymatic activity and DHA production observed for mutant strain I-2-239.

Combined mutagenesis, including UV irradiation, atmospheric and room temperature plasma, and ion beam implantation, was employed to improve the productivity

Table 3. Glycerol-oxidizing activity of intact cells of strains L-6 and I-2-239.

Microorganisms	Activity (mmol DHA/h)
L-6	0.19 ± 0.05
I-2-239	0.34 ± 0.05

Table 4. Sites of mutation in GLDH of strain I-2-239 relative to wild strain L-6.

Polypeptide	Nucleotide	Position	Amino acid	Position
sldB	C → T	82	L → F	28
	C → T	314	P → L	105
	C → T	323	P → L	108
sldA	A → G	391	T → A	131
	G → A	459		
	T → C	808	S → P	270
	C → T	866	P → L	289
	A → G	1091	Y → C	364
	A → T	1100	Q → L	367
	T → C	1301	I → T	434
	C → T	1660	H → Y	554

of DHA by *G. oxydans*. The starting strain with a DHA productivity of 47.98 mg/ml was screened from a soil sample. After step-by-step mutagenesis, DHA productivity of the ultimate mutant strain I-2-239 was dramatically increased. In shake-flask fermentation, DHA productivity of 103.5 g/l was achieved by the mutant strain with a starting glycerol concentration of 120 g/l, which was 115.7% higher than the wild strain. The culture time was also reduced from 54 h to 36 h. Comparative investigation between the starting strain and the mutant strain indicated that the mutations did not significantly affect biomass; however, much higher growth rate and enzyme activity were observed for the mutant strain. The 3-D structure of sldA in the wild strain was modeled using I-TASSER, and the active site residue and PQQ binding site residues were also predicted. Among the 10 amino acid substitutions identified in the mutant sldA polypeptide by sequence alignment, amino acid residue 289 was included in the predicted PQQ binding sites and several other residues were very close to the predicted sites. It was speculated that these mutations improved PQQ binding and thus the enzyme activity. The increased transcription level of both *sldA* and *sldB* was also assumed as one of the underlying reasons for the increased enzyme activity and DHA productivity in the mutant strain.

Acknowledgments

This study was supported by "111 Project" from the Ministry of Education of China and State Administration of Foreign Experts Affairs of China (No. 111-2-07). This study was also supported by A Project Funded by the Priority Academic Program Development of Jiangsu Higher Education Institutions.

References

1. Ameyama M, Matsushita K, Ohno Y, Shinagawa E, Adachi O. 1981. Existence of a novel prosthetic group, PQQ, in membrane-bound, electron transport chain-linked, primary dehydrogenases of oxidative bacteria. *FEBS Lett.* **130:** 179-183.
2. Ameyama M, Shinagawa E, Matsushita K, Adachi O. 1985. Solubilization, purification and properties of membrane-bound glycerol dehydrogenase from *Gluconobacter industrius*. *Agric. Biol. Chem.* **49:** 1001-1010.
3. Bicker M, Endres S, Ott L, Vogel H. 2005. Catalytical conversion of carbohydrates in subcritical water: a new chemical process for lactic acid production. *J. Mol. Catal. A Chem.* **239:** 151-157.
4. Black CS, Nair GR. 2013. Bioconversion of glycerol to dihydroxyacetone by immobilized *Gluconacetobacter xylinus* cells. *Int. J. Chem. Eng. Appl.* **4:** 310-314.
5. Brenner DJ, Krieg NR, Staley JT, Garrity GM. 2005. Genus VIII. *Gluconacetobacter*, pp. 72-73. *In* Brenner DJ, Krieg NR, Staley JT (eds.), *Bergey's Manual of Sytematic Bacteriology*, 2nd Ed. Springer Science+Business Media, New York.
6. Chen J, Chen JH, Zhou CL. 2008. HPLC method for determination of dihydroxyacetone and glycerol in fermentation broth and comparison with a visible spectrophotometric method to determine dihydroxyacetone. *J. Chromatogr. Sci.* **46:** 912-916.
7. Enders D, Voith M, Lenzen A. 2005. The dihydroxyacetone unit – a versatile C(3) building block in organic synthesis. *Angew. Chem. Int. Ed. Engl.* **44:** 1304-1325.
8. Gätgens C, Degner U, Bringer-Meyer S, Herrmann U. 2007. Biotransformation of glycerol to dihydroxyacetone by recombinant *Gluconobacter oxydans* DSM 2343. *Appl. Microbiol. Biotechnol.* **76:** 553-559.
9. Guo T, Tang Y, Xi YL, He AY, Sun BJ, Wu H, *et al*. 2011. *Clostridium beijerinckii* mutant obtained by atmospheric pressure glow discharge producing high proportions of butanol and solvent yields. *Biotechnol. Lett.* **33:** 2379-2383.
10. Hekmat D, Bauer R, Fricke J. 2003. Optimization of the microbial synthesis of dihydroxyacetone from glycerol with *Gluconobacter oxydans*. *Bioprocess Biosyst. Eng.* **26:** 109-116.
11. Hekmat D, Bauer R, Neff V. 2007. Optimization of the microbial synthesis of dihydroxyacetone in a semi-continuous repeated-fed-batch process by in situ immobilization of *Gluconobacter oxydans*. *Process Biochem.* **42:** 71-76.
12. Hoshino T, Sugisawa T, Shinjoh M, Tomiyama N, Miyazaki T. 2003. Membrane-bound D-sorbitol dehydrogenase of *Gluconobacter suboxydans* IFO 3255 – enzymatic and genetic characterization. *Biochim. Biophys. Acta* **1647:** 278-288.
13. Hu ZC, Liu ZQ, Xu JM, Zheng YG, Shen YC. 2012. Improvement of 1,3-dihydroxyacetone production from *Gluconobacter oxydans* by ion beam implantation. *Prep. Biochem. Biotechnol.* **42:** 15-28.
14. Hu ZC, Zheng YG. 2009. A high throughput screening method for 1,3-dihydroxyacetone-producing bacterium by cultivation in a 96-well microtiter plate. *J. Rapid Methods Autom. Microbiol.* **17:** 233-241.
15. Hu ZC, Zheng YG. 2011. Enhancement of 1,3-dihydroxyacetone production by a UV-induced mutant of *Gluconobacter oxydans* with DO control strategy. *Appl. Biochem. Biotechnol.* **165:** 1152-1160.
16. Lapenaite I, Kurtinaitiene B, Razumiene J, Laurinavicius V, Marcinkeviciene L, Bachmatova I, *et al*. 2005. Properties and analytical application of PQQ-dependent glycerol dehydrogenase from *Gluconobacter* sp. 33. *Anal. Chim. Acta* **549:** 140-150.
17. Li G, Li HP, Wang LY, Wang S, Zhao HX, Sun WT, *et al*. 2008. Genetic effects of radio-frequency, atmospheric-pressure glow discharges with helium. *Appl. Phys. Lett.* **92:** 221504.
18. Liu RM, Liang LY, Ma JF, Ren XY, Jiang M, Chen KQ, *et al*.

2013. An engineering *Escherichia coli* mutant with high succinic acid production in the defined medium obtained by the atmospheric and room temperature plasma. *Process Biochem.* **48:** 1603-1609.
19. Liu YP, Sun Y, Tan C, Li H, Zheng XJ, Jin KQ, Wang G. 2013. Efficient production of dihydroxyacetone from biodiesel-derived crude glycerol by newly isolated *Gluconobacter frateurii. Bioresour. Technol.* **142:** 384-389.
20. Ma L, Lu W, Xia Z, Wen J. 2010. Enhancement of dihydroxyacetone production by a mutant of *Gluconobacter oxydans*. *Biochem. Eng. J.* **49:** 61-67.
21. Miyazaki T, Tomiyama N, Shinjoh M, Hoshino T. 2002. Molecular cloning and functional expression of D-sorbitol dehydrogenase from *Gluconobacter suboxydans* IFO3255, which requires pyrroloquinoline quinone and hydrophobic protein SldB for activity development in *E. coli. Biosci. Biotechnol. Biochem.* **66:** 262-270.
22. Nabe K, Izuo N, Yamada S, Chibata I. 1979. Conversion of glycerol to dihydroxyacetone by immobilized whole cells of *Acetobacter xylinum*. *Appl. Environ. Microbiol.* **38:** 1056-1060.
23. Nie GJ, Yang XR, Liu H, Wang Li, Gong GH, Jin W, Zheng ZM. 2013. N^+ ion beam implantation of tannase-producing and *Aspergillus niger* and optimization of its process parameters under submerged fermentation. *Ann. Microbiol.* **63:** 279-287.
24. Raška J, Skopal F, Komers K, Machek J. 2007. Kinetics of glycerol biotransformation to dihydroxyacetone by immobilized *Gluconobacter oxydans* and effect of reaction conditions. *Collect. Czech. Chem. Commun.* **72:** 1269-1283.
25. Roy A, Kucukural A, Zhang Y. 2010. I-TASSER: a unified platform for automated protein structure and function prediction. *Nat. Protoc.* **5:** 725-738.
26. Ruch FE, Lin EC. 1975. Independent constitutive expression of the aerobic and anaerobic pathways of glycerol catabolism in *Klebsiella aerogenes. J. Bacteriol.* **124:** 348-352.
27 Silva GPD, Mack M, Contiero J. 2009. Glycerol: a promising and abundant carbon source for industrial microbiology. *Biotechnol. Adv.* **27:** 30-39.
28. Toyama H, Chen ZW, Fukumoto M, Adachi O, Matsushita K, Mathews FS. 2005. Molecular cloning and structural analysis of quinohemoprotein alcohol dehydrogenase ADH-IIG from *Pseudomonas putida* HK5. *J. Mol. Biol.* **352:** 91-104.
29. Wang LY, Huang ZL, Li G, Zhao HX, Xing XH, Sun WT, *et al*. 2009. Novel mutation breeding method for *Streptomyces avermitilis* using an atmospheric pressure glow discharge plasma. *J. Appl. Microbiol.* **108:** 851-858.
30. Wang Q, Feng LR, Wei L, Li HG, Wang L, Zhou Y. 2014. Mutation breeding of lycopene-producing strain *Blakeslea trispora* by a novel atmospheric and room temperature plasma (ARTP). *Appl. Biochem. Biotechnol.* **174:** 452-460.
31. Xu S, Wang X, Du G, Zhou J, Chen J. 2014. Enhanced production of L-sorbose from D-sorbitol by improving the mRNA abundance of sorbitol dehydrogenase in *Gluconobacter oxydans* WSH-003. *Microb. Cell Fact.* **13:** 146.
32. Yang J, Yan R, Roy A, Xu D, Poisson J, Zhang Y. 2014. The I-TASSER Suite: protein structure and function prediction. *Nat. Methods* **12:** 7-8.
33. Yang J, Zhang Y. 2015. I-TASSER server: new development for protein structure and function predictions. *Nucleic Acids Res.* **43:** 174-181.
34. Yang W, Zhou Y, Zhao ZK. 2013. Production of dihydroxyacetone from glycerol by engineered *Escherichia coli* cells co-expressing *gldA* and *nox* genes. *Afr. J. Biotechnol.* **12:** 4387-4392.
35. Zong H, Zhan Y, Li X, Peng L, Feng F, Li D. 2012. A new mutation breeding method for *Streptomyces albulus* by an atmospheric and room temperature plasma. *Afr. J. Microbiol. Res.* **6:** 3154-3158.